SCIENCE CHINA
Information Sciences

• RESEARCH PAPERS •
Special Focus

March 2011 Vol. 54 No. 3: 577–588
doi: 10.1007/s11432-010-4086-6

Closed-loop drip irrigation control using a hybrid wireless sensor and actuator network

LI Zhen[1,2], WANG Ning[2], HONG TianSheng[1]*, FRANZEN Aaron[2] & LI JiaNian[1]

[1]*Key Laboratory of Key Technology on Agricultural Machinery and Equipment of South China Agricultural University, Ministry of Education, Guangzhou* 510642*, China;*
[2]*Department of Biosystems and Agricultural Engineering, Oklahoma State University, Stillwater, OK,* 74078*, USA*

Received May 7, 2010; accepted August 20, 2010; published online October 1, 2010

Abstract In this research, a closed-loop drip irrigation control hybrid wireless sensor and actuator network (HWSAN) prototype were developed and deployed in a crop field for soil property precise measurement and precision irrigation in accordance with the measured soil property. The HWSAN was composed of a wireless sensor and actuator network (WSAN) used for in-field soil property monitoring and irrigation control and a laboratory supervising system. The WSAN included ten sensor nodes, five irrigation control nodes, a central node, a gateway and a cellular modem. The laboratory supervising system was formed by a web-server. The system could automatically sample soil properties including soil moisture, electrical conductivity, and near-surface temperature at four different depths underground and transmit field data through cellular network to the web-server. Closed-loop control was achieved through the control nodes listening uploading packets from its paired sensor nodes to control drip irrigation. Results from the quality of service (QoS) evaluation included: the data packet transmission rate was 84.76%, data accuracy rate was greater than 97% and no in-field data transmission errors.

Keywords wireless sensor network, drip irrigation, soil property monitoring, precision agriculture

Citation Li Z, Wang N, Hong T S, et al. Closed-loop drip irrigation control using a hybrid wireless sensor and actuator network. Sci China Inf Sci, 2011, 54: 577–588, doi: 10.1007/s11432-010-4086-6

1 Introduction

A reliable automatic, real-time and continuous closed-loop irrigation control system integrates soil property monitoring, irrigation scheduling and control for remote and large agricultural fields. It has advantages on labor cost, plant stress levels and natural resource consumption over traditional methods, with which soil property monitoring and irrigation actuation were often loosely coupled due to a lack of efficient communication links in between.

In the case of soil property monitoring, recent successful exploring efforts have revealed great adaptability of wireless sensor network (WSN) technology for in-field data collection. Monitored parameters ranges from temperature, humidity, rain fall, wind speed, and solar radiation within micro-climate to those soil properties such as moisture, electrical conductivity, and near surface temperature as well as

*Corresponding author (email: tshong@scau.edu.cn)

those for water qualities like sediment runoff and pollution concentration [1–7]. However, most of them are still used for sensing, but seldom for controls and actuations [8–10].

In this research, a two-tier hybrid wireless sensor and actuator network (HWSAN) was developed to acquire field soil property data and control drip irrigation. The ultimate goal was to integrate an autonomous drip irrigation control system with an in-field soil property monitoring wireless sensor network. The system should provide researchers and users real-time soil property information, irrigation control status, and allow the data to be accessed online from a dedicated website. The specific objectives of the research included: 1) To design and develop a distributed data acquisition system based on HWSAN for unattended field-specific soil property monitoring; 2) to integrate an irrigation control system with the in-field WSAN for automated closed-loop variable-rate drip irrigation; 3) to deploy the HWSAN into a crop field; and 4) to test the quality of service (QoS) of the developed HWSAN system under laboratory and field conditions, respectively.

2 Method and materials

The HWSAN developed for monitoring in-field soil property variability and controlling the closed-loop variable-rate drip irrigation included two tiers of: 1) an in-field local wireless sensor and actuator network (LWSAN) for soil property data acquisition and irrigation control; and 2) a long range cellular communication network (LRCN) for uploading in-field data to a lab web-server providing off-line soil property data storage, curving and analysis

2.1 System design for the LWSAN

Since the LWSAN was intended for un-supervised in-field applications, the wireless sensor network had to be simple but robust enough to operate in harsh conditions without excessive human interference. A single-hop networking cluster with star-topology allowed direct communication between the central nodes. Each sensor node inside one cluster is free of complex routing and routing table maintenance which usually required up to five minute interval [11]. Figure 1 shows the field installation of the LWSAN forming a single-hop networking cluster with star-topology. The LWSAN included a central node and ten sensor nodes working together to collect real-time soil property data. Five irrigation control nodes were deployed into the field passively receiving uploaded soil property data packets from its paired sensor nodes to start and stop the site-specific drip irrigation without excessively disturbing the monitoring system.

The physical locations of the nodes were predefined before deployment based on previous knowledge of soil variability and remained stable unless a network reconfiguration was implemented. At each location, a sensor node acquired hourly soil property data including soil surface temperature, electrical conductivity, and soil moisture content and wirelessly transmitted them to the central node boxed together with the gateway for a temporary storage. The data stored in the central node would be uploaded to a gateway based on its request through wireless communications. Each of the five irrigation control nodes was paired with the sensor node closest to it in physical location and was assigned a unique node ID. The irrigation control nodes could either start or stop drip irrigation based on a preset time interval and duration or control the irrigation passively based on received soil property monitoring packets from its paired sensor node, compare the soil moisture level with a predefined threshold, and start or stop irrigation.

2.1.1 *Sensor node configuration*

Figure 2 depicts the major components within a sensor node. IRIS motes (IRIS, Crossbow Technology Inc., San Jose, CA, USA) were used as the wireless control and communication kernel. Major specifications of an IRIS mote were: 2405 to 2480 MHz ISM band programmable in 1 MHz steps, up to 250 kbps transit data rate, −101 dBm receive sensitivity, 8k bytes RAM.

Capacitancebased soil moisture sensors, namely EC-5 (ECH2O probe, Model EC-5, Decagon Devices, Pullman, MA, USA) were applied for taking underground volumetric water content (VWC). The total

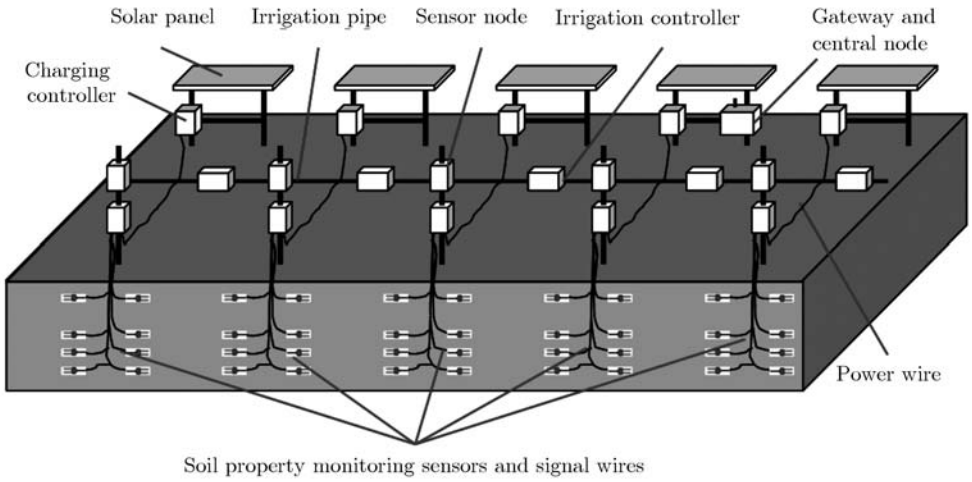

Figure 1 Field deployment of the LWSAN.

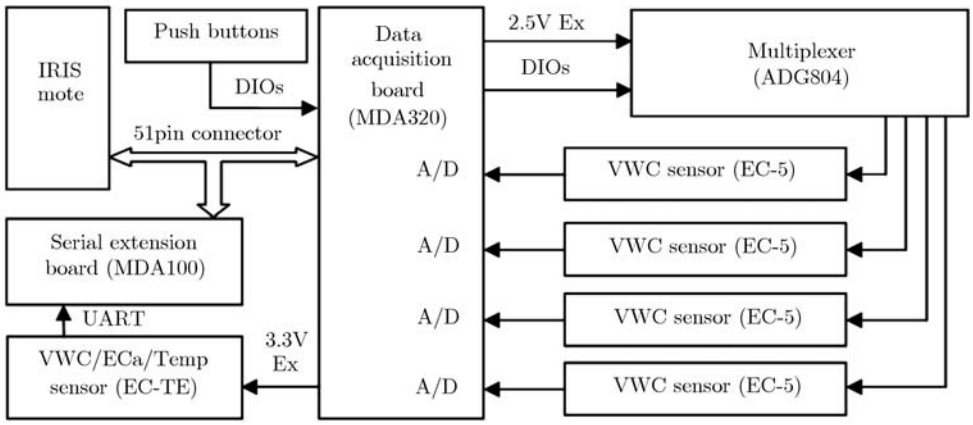

Figure 2 Block diagram of major components in a sensor node.

volume of influence (maximum possible measurement volume) of the EC-5 was approximately 181 cm^3. EC-5 was calibrated based on local soil texture in the previous study [7]. EC-TE sensors (Model ECH2O-TE, Decagon Devices, Pullman, MA, USA) were used to measure volumetric water content, temperature, and bulk electrical conductivity of soil and growing media. Once activated, the EC-TE sensor output a packet including three numerical data related to VWC, bulk electrical conductivity (EC), and temperature. The data packet was transmitted in an ASCII format with a dynamic length using 1200 baud serial communication to the IRIS mote. In the data packet, the first numerical data was related to VWC readings which fell to a range from approximately 400 to 1300.

Raw electrical conductivity reading (σ_{raw}) from EC-TE was valid in the range from 0 to 1022. σ_{raw} could be converted to bulk electrical conductivities in dS/m using eq. (1). The EC reading was temperature corrected within the EC-TE probe:

$$EC = \begin{cases} \dfrac{\sigma_{\text{raw}}}{100}, & \sigma_{\text{raw}} \leqslant 700, \\ \dfrac{700 + 5(\sigma_{\text{raw}} - 700)}{100}, & \sigma_{\text{raw}} > 700, \end{cases} \tag{1}$$

where EC was the bulk electrical conductivity in dS/m and σ_{raw} was the raw electrical conductivity reading received from an EC-TE probe.

The third data was corrected temperature reading T_1 in Celsius. The correction function is as follows:

$$T_1 = 10 \times T + 400, \tag{2}$$

where T_1 is the transmitted temperature reading and T is the real temperature reading in °C with one decimal precision

A multi-functional data acquisition board (MDA320, Crossbow Technology Inc., San Jose, CA, USA) was connected to an IRIS mote through a 51-pin extension connector. Four single-ended 0–2.5 V analog input channels were used to read data from four EC-5 sensors. Three digital I/Os were used for enabling and selecting channels on the multiplexer while another two for responding to push buttons. MDA320 also provided 2.5 and 3.3 V excitations to activate EC-5 and EC-TE sensors, respectively. All the on-going communication between IRIS and MDA320 went through I2C interface. Another data acquisition (DAQ) board (MDA100, Crossbow Technology Inc., San Jose, CA, USA) was connected with the IRIS mote through the same 51-Pin connector to provide an UART interface to acquire data from the EC-TE sensor.

Together with the 2.5 V excitation channel on MDA320, a multiplexer, ADG804 (Analog Device, Inc., Norwood, MA, USA) was used to power up the EC-5 sensors. The input of the multiplexer was connected to the MDA320's 2.5 V excitation output. The output channels of the multiplexer were selected sequentially to excite one EC-5 sensor a time. The EC-TE was directly powered by the 3.3 V excitation of MDA320.

2.1.2 *Sensor node packaging and installation*

Each sensor node was packaged in a weather-proof plastic container. Two sensor nodes were mounted at 1.5 to 2.0 m above ground on a steel pole installed at the edges of field strips. Two pushbuttons were connected to two digital I/Os on the MDA320. One of the buttons, if pressed, would activate an immediate soil property sampling and data transmission. The other one would initiate an uploading of the restored data from a sensor node's local memory to a base node. All antennas on sensor nodes were adjusted to face to the central node and maintained for line-of-sight communications.

Each sensor node was connected to four soil property sensors implanted at four different depths as 5.08, 15.24, 30.48 and 60.96 cm underground. The lower three were all EC-5 sensors while the top one could be either EC-5 or EC-TE. Currently, five of the sensor nodes were using EC-5 while the other five were using EC-TE.

2.1.3 *Central node configuration*

The central node was boxed together with the gateway and formed by an IRIS mote with a 512 kB flash for data storage. It was responsible for collecting and storing measurement data received from each sensor node and uploading the stored data to the gateway on request. The current address assignment was sufficient for restoring up to 210 day's data plus a ten-packet space for buffering incoming packets during data upload. Once a datum was uploaded, its space in the flash was cleared and refilled by new datum

2.1.4 *Power station configuration*

Currently, five power supply units were deployed on the edges of the strips. Each of the units was providing energy to two sensor nodes while one of them was also supporting the central node and the gateway. Each sensor node's power consumption and duration were measured and calculated through lab tests based on the sampling rate of one sample/hour. The central node and gateway's power consumption was obtained through lab tests based on one power cycle (or communication link establishment) per hour.

A 12 V 12 Ah Lead-Acid heavy-duty battery (CF-12V12, Eagle Picher Technologies, Joplin, MO, USA) was selected based on requirements and measurement results: 1) the cellular modem needed a 3.25 W power for operation; 2) to guarantee the WSN system operation in snow season at Stillwater, Oklahoma during which solar panels may be covered by snow and the in-field system would be un-reachable for several days; and 3) to reserve power supply ability for more nodes in network expansion. A 15 W solar panel (Northern Industrial, Burnsville, MN, USA) was selected to provide enough peak voltage to the 12 V battery during charging and current which could replenish the energy consumed by the nodes and the

gateway. The cellular modem was directly powered by the battery while the rest of the components were supported through a 3.3 V 1 A regulator.

To conserve power and extend battery life, a sensor node was turned into idle mode and the radio on it was disabled most of the time. It was enabled just for a short period to upload the data and detect the commands from the central node or gateway. This power management strategy was achieved with the sensor node software.

The gateway was packed together with a power controller which turned off power supply to both the Stargate mother board and the cellular modem most of the time during a day and turned it on hourly for a short time for communications. If there was no incoming communication within 10 s, the gateway will turn itself off until next hour.

The central node was kept in idle mode with only the radio turned on for incoming data packages from the sensor nodes. No pre-synchronization was needed for each communication link establishment.

Power management evaluation was performed in the lab before system deployment using one sensor node, the central node, and the gateway. Each of the components worked exactly the same as they were in the field. Current consumption of the sensor node, central node and gateway were measured by reading the voltage drops across three 10 Ω resistors placed in series with either the power regulator for a sensor node or central node or the 12 V battery for the gateway. The resistors had relatively larger values compared to typical current-sensing resistors (typically 1 Ω) for measuring small current without inducing low-voltage problems [11]. Voltage drop at each resistor was monitored and recorded using a data-logger (CR3000, Campbell Scientific, Logan, UT, USA). Each channel's data-sampling rate was 5 ms for capturing current consumption during power cycling, data acquisition, buttoned procedures, and radio operations.

2.1.5 *Irrigation control node configuration*

Figue 3 depicts the major components within an irrigation control node. An ATMega8L (Atmel Ltd., California, USA) microprocessor was applied as the control unit. Major characteristics of the processor included: 8K bytes programmable flash memory, 512 bytes EEPROM and 1K internal SRAM. Drip irrigation was started and stopped by controlling a 5 V electromagnetic valve which was electrically connected with an electromagnetic valve driver and physically connected with the water supply pipes. The electromagnetic valve driver was connected to the micro-processor and used to enhance the control signals to the valve.

Wireless communication between the irrigation control node and its paired sensor node was achieved through a 2.4 GHz ZigBee compatible module (LM2400, RadioPulse Inc., Korea). The module was compatible with Zigbee and IEEE 802.15.4 standards and integrated 2.4 GHz RF transceiver, PHY, modem, MAC and an 8 bit MCU into a single chip. It operated at 1.5 V and had programmable transmit power of up to +7 dBm. The module was connected to the ATMega8L micro-processor through a UART interface.

Timing was achieved by using a trickle-charger timekeeping real time clock chip (RTC, DS1302, Dallas Semiconductors, California, USA). The RTC counted seconds, minutes, hours, date of the month, month, day of the week, and year with leap-year compensation valid up to year 2100. The RTC communicated with the micro-processor through I2C interface. Timing could be kept though a 3.6 V button battery if the major power supply failed.

Each irrigation control node was packaged in a weather-proof plastic container. The knob switch and the dedicated keys in the front panel worked together to adjust irrigation timing and duration. The LEDs displayed working modes or indicated steps in setting irrigation timing and duration. The irrigation control nodes were powered independently by a 9 V battery, hence, would not influence the power supply of other nodes. Each irrigation control node was installed on the ground beside water pipes and between its paired sensor node and the power station.

The embedded program working inside the irrigation control nodes could adjust automatically between the two operation modes: independent mode and networked mode.

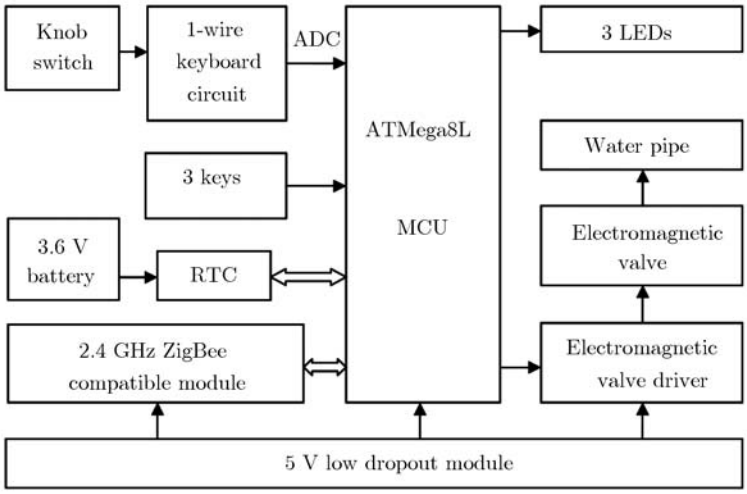

Figure 3 Major components within an irrigation control node.

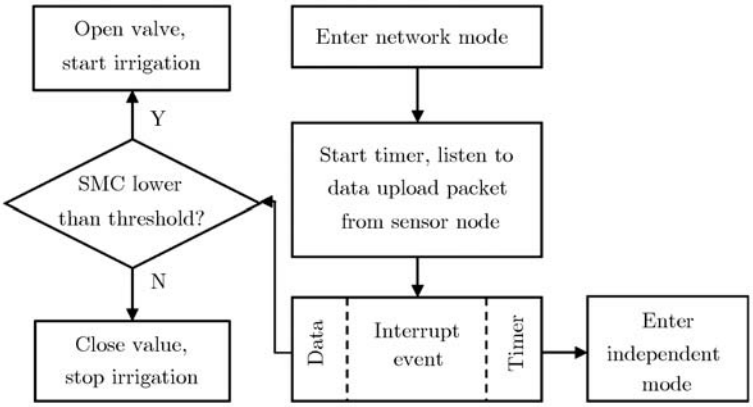

Figure 4 Flow chart of irrigation control node under the networked mode.

• Independent mode. The Independent mode was the basic mode of a control node. Once deployed, by default the system was initiated to work in the independent mode. When the control node was working under this mode, it started and stopped the drip irrigation based on a user defined time interval and duration daily by controlling an electromagnetic valve (FD-18C, Fuxin Ltd., Zhejiang, China) connected with both the control node and water pipes in the field.

• Networked mode. Under networked mode, a control node listened to its paired sensor node to acquire the soil property information, compared the acquire information with the predefined threshold stored in the Flash, and sent a control command to a valve. If there was no data upload packet received for a specified time interval, the control node would autonomously enter independent mode. The flow chart of irrigation control scheme under the networked mode was depicted in Figure 4.

2.1.6 *Sensor node embedded system design*

All the programs for wireless sensor network communications within the system were developed under the TinyOS 1.1 environment which fully supporting the IRIS mote and two DAQs used in this research. A TinyOS application was implemented as a set of component modules written in a C extension language, namely NesC.

The sensor node program was embedded in the IRIS mote and controlled the component activities of the IRIS mote, two DAQs, the multiplexer, and the radio transceiver. These activities included hourly sampling, recording and storing soil property data, transmitting the data wirelessly to the central node, and reserved for controlling corresponding irrigation control node. For immediate data uploading purpose,

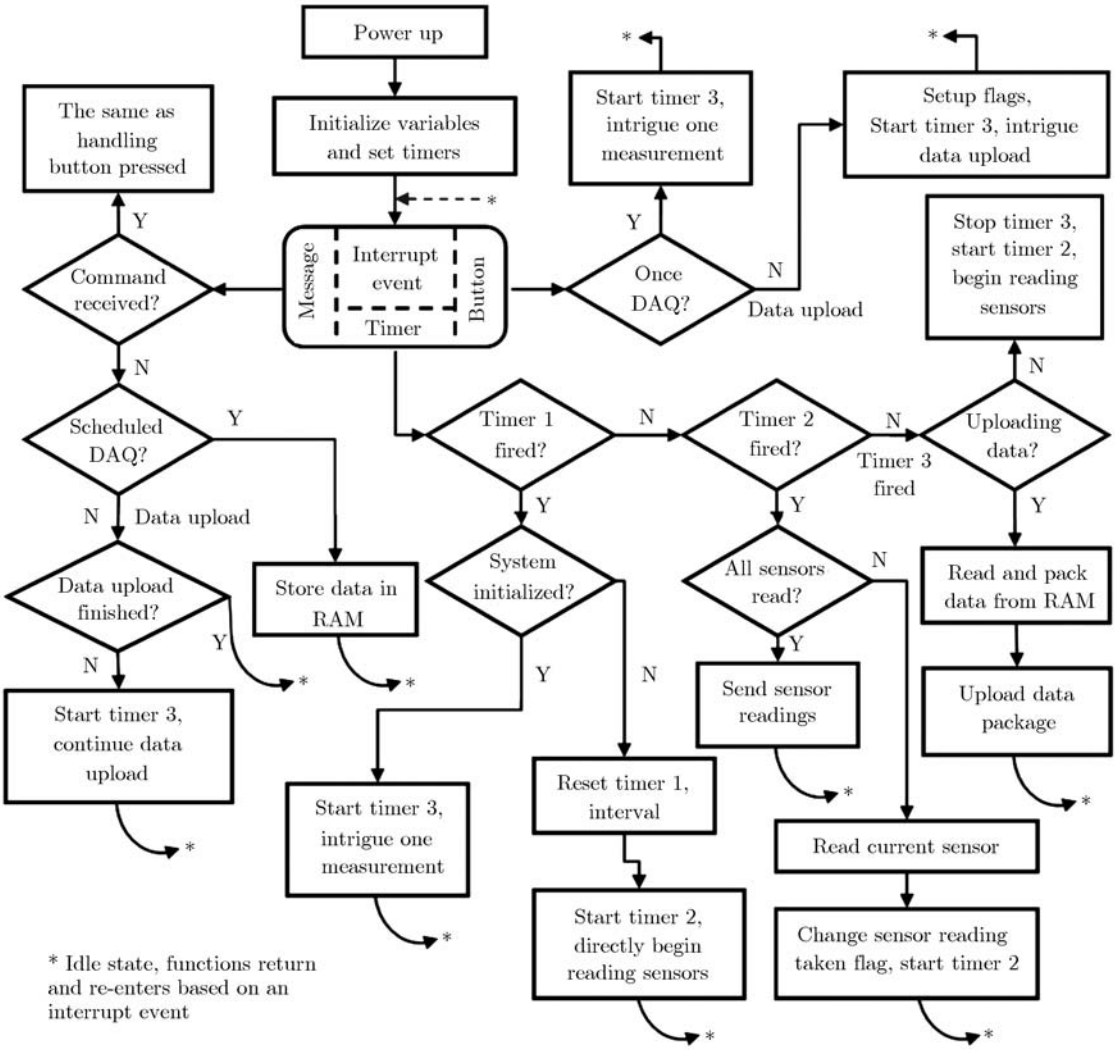

Figure 5 Flow chart for the sensor node program structure.

the sensor node was able to respond the requests either from the push buttons on the sensor node box, the central node, or a mobile base node with pre-defined commands. The sensor node program allowed autonomously detection of the sensor type installed at the depth of 5.08 cm (EC-5 or EC-TE). If no EC-TE was detected, the program skipped the EC-TE measurement process, directly entered the EC-5 measurement procedures, and filled zeros to the fields for EC-TE measurement within a data packet. Flow chart of the sensor node program structure using TinyOS components is depicted in Figure 5.

In TinyOS 1.1, applications are classified into two levels as "task" and "event". A "task" is usually invoked in applications with low real-time requirements. There is no priority between different tasks so that they are handled using the FIFO strategy unless one task is paused and release the CPU. The "events", mostly interrupts on the other hand, can break a task and be processed immediately. However, new tasks generated by events have to be put into the end of the FIFO buffer and processed after all the previous tasks. If there is no task or event, the CPU enters Idle/Sleep mode autonomously to save energy.

Advantages of the scheduling mechanism used in TinyOS 1.1 are: 1) suitable for normal WSN platforms with limited system resources; 2) low power consumption; and 3) high concurrency.

2.1.7 *In-field wireless communication protocol*

The in-field star-topology wireless communications included: 1) sensor nodes to the central node; 2) a sensor or the central node to the base node; and 3) the base node to a sensor or the central node. The

Table 1 Data fields within a protocol data unit (PDU) for a soil property measurement

Field name	Field size	Description	
Node ID	1 byte	Indicating packet origination or destination depending on packet type	
Index	2 bytes	Sequential packet identifier	
Packet type	1 byte	0x00	Data packet, central or sensor node to base data upload, Node ID indicates origination
		0x01	Data packet, sensor node to central node data upload, Node ID indicates origination
		0x02	Command packet, base to central or sensor node command, Node ID indicates destination
		0x03	Command packet, sensor node to irrigation control node to start or stop irrigation, Node ID indicates destination
EC-5-a	2 bytes	Soil moisture reading of EC-5 at the depth of 60.96 cm	
EC-5-b	2 bytes	Soil moisture reading of EC-5 at the depth of 30.48 cm	
EC-5-c	2 bytes	Soil moisture reading of EC-5 at the depth of 15.24 cm	
EC-5-d	2 bytes	Soil moisture reading of EC-5 at the depth of 5.08 cm	
VWC	2 bytes	Measured VWC reading of EC-TE*	
EC	1 byte	Electrical conductivity reading of EC-TE*	
Temp	2 bytes	Temperature reading of EC-TE*	

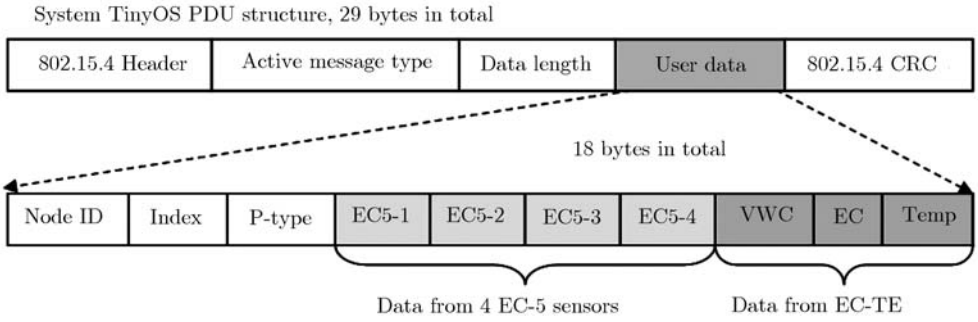

Figure 6 Format of the TinyOS protocol data unit (PDU).

base node could be either a stable base node connected to the gateway or a mobile base node for on-the-go data acquisition connected to a laptop PC. User data structures were designed to be uniform for different types of communication. The total length of the user data segment was 18 bytes. Names, size, and descriptions of each field within the user data segment of a PDU are explained in Table 1.

Messages for in-field wireless communication between different nodes were nested as the "User data" field based on the TinyOS standardized protocol data unit (PDU). A complete packet for the in-field WSN communication was depicted in Figure 6.

2.2 System design for the LRCN

2.2.1 *Gateway configuration*

The gateway was composed of a Stargate board (SPB400CB, Crossbow Technology Inc., San Jose, USA), a Stargate communication extension daughter board (SDC400CA, Crossbow Technology Inc., San Jose, USA), an IRIS mote as the base node, and a CF card. The gateway was packed together with a power supervisory controller, the central node, and a cellular modem (MTCBA-G-G4, MultiTech, USA) in a weather proof box.

2.2.2 *Data uploading protocol between the central node and the gateway*

After waked up from a power loop, the gateway sent data-upload requests wirelessly to the central node. If there were measurement data stored in the flash, the central node would enter Uploading mode

and start uploading data to the gateway. To guarantee no packet loss during the data uploading, an acknowledgement packet (ACK) was returned from the gateway after receiving each packet. Once the central node finished sending a packet, a 10-s time-out routine was activated. If an ACK was not received before the time-out, the central node exited the Uploading mode and maintained the last uploaded packet. Otherwise, the central node cleared the last packet and started uploading a new one.

2.2.3 *The central node program*

A central node worked at three states: Normal, Uploading, and Renewing. At "Normal" state, the central node stored measurement data received from the sensor nodes to its on-board flash and waited for a data uploading request from the gateway. "Uploading" was the state at which the central node uploaded the data in the flash to the gateway through a wireless radio link. "Renewing" was the state at which the data packets were transferred from temporary buffer to the regular storage. The temporary buffer was a consecutive data storage area with a capacity of restoring ten packets in the central node's on-board flash. If any packets from the sensor nodes arrived at the central node when it was in the Uploading mode, these packets would be saved to the temporary buffer. After exiting the Uploading mode, the central node would check whether or not there was any packet in the temporary buffer and enter Renewing mode if needed. The maximum time for a central node to remain in Renewing state was about 110 ms and an assumption was made that there was no incoming communication during this time within a sampling interval of one hour.

3 HWSAN system quality of service (QoS) evaluation

3.1 Data transmission performance test

In-field vegetation led to physical signal attenuation and packet competition introduced logical failures, both of which influences greatly on system stability. The indexed packets from each sensor node arrive at the web-server every day during a certain period (between May 4th and June 10th, 2009) were recorded as shown in Figure 7. Total packets sent from each node during that period were calculated from the subtraction of the last and first received packet index inside database. A packet delivery rate ($N_{R,pdr}$) was defined as

$$N_{R,pdr} = \frac{Nr}{Nt} \times 100\%, \tag{3}$$

where Nt was the packet transmitted in a certain period of time by one sensor node and Nr was the packet arrived at data base during the same period from the same node.

It could be seen from Figure 7 that except for node 2, the rest of the nodes worked properly during the period of test since their daily number of packets received was around 24 for each node. For node 2, the sudden increase happened due to another system test carried out on May 16th, 2009 using that node which in return led to a frequent reset of the node and thus made the number of packets arrive at the data-base much larger than that of normal monitoring operations. Data transmission performance evaluation results are displayed in Table 2. The averaging system $N_{R,pdr}$ was 84.76% while the $N_{R,pdr}$ of sensor node 2 was excluded for its extra low reading since sensor node 2 was located at the furthest distance from the central node and was mostly influenced by the plant canopy attenuation.

3.2 System reliability

Results contained invalid values due to protocol failure of TinyOS 1.1. Each invalid data were marked "NULL" within the database and excluded from graphic generating. A valid data rate ($N_{R,val}$) was defined as

$$N_{R,val} = \frac{Nv}{Nr} \times 100\%, \tag{4}$$

where Nr was the number of packets arriving during a certain period of time (between May 4th and May 14th, 2009) of one sensor station and Nv was the number of valid data of each sensor within one sensor node during the same time. System reliability performance test results were as shown in Table 3. The

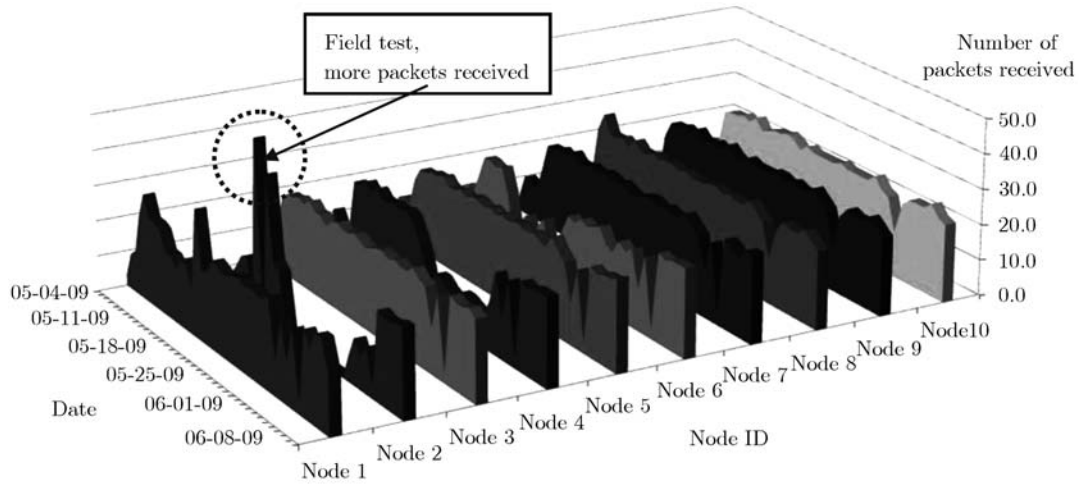

Figure 7 Number of packets received daily from each sensor node.

Table 2 Results of data transmission evaluation

Node ID	1	2	3	4	5	6	7	8	9	10
PDR(%)	89.2	31.9	90.6	68.2	90.3	94.4	90.2	97	98.4	97.4

Table 3 Number of packets received daily from each sensor node

Node ID	$N_{R,val}$ (%)						
	EC5-1	EC5-2	EC5-3	EC5-4*	VWC*	EC*	Temp*
1	98.5	98.5	100	100	N/A	N/A	N/A
2	100	98.2	100	100	N/A	N/A	N/A
3	99.0	99.5	98.0	98.5	N/A	N/A	N/A
4	98.9	98.9	100	98.9	N/A	N/A	N/A
5	99.5	99	99.5	99.0	N/A	N/A	N/A
6	100	99.4	100	N/A	100	100	99.4
7	99.5	99.5	100	N/A	99.5	100	98.9
8	100	95.7	99.0	N/A	100	100	100
9	100	98.9	99.5	N/A	97.8	100	100
10	99.0	100	99	N/A	91.9	100	100
Average	99.4	98.8	99.5	99.3	97.8	100	99.7

*Sensor Nodes 1 to 5 did not have EC-TE thus the $N_{R,val}$ for EC-TE are N/A; sensor nodes 6 to 10 did not have EC5-4, thus the readings were N/A.

minimum valid data rate was 91.9% obtained in Node 10 while the majority (49 out of 50) valid data rates of sensors in each sensor node were above 97%.

3.3 In-field data error rate

The in-field data error rate was defined to determine whether or not and to what extent the differences were between data coming in and out of the central node. An extra pseudo sensor station (named Node 21) with only an IRIS and an MDA320 was programmed to send PDUs in a shortened time interval as 10 s. A mobile base node connected to a laptop was applied to supervise communication in and out of the central node. Test duration was limited in between two central node data uploads since the extra buffer for central node to use in Uploading mode was only 10 packets. Data error rate ($N_{R,err}$) was calculated using

$$N_{R,err} = \frac{Ne}{Nt} \times 100\%, \tag{5}$$

where Nt was the total number of PDU transmitted by the pseudo station and Ne was the number of

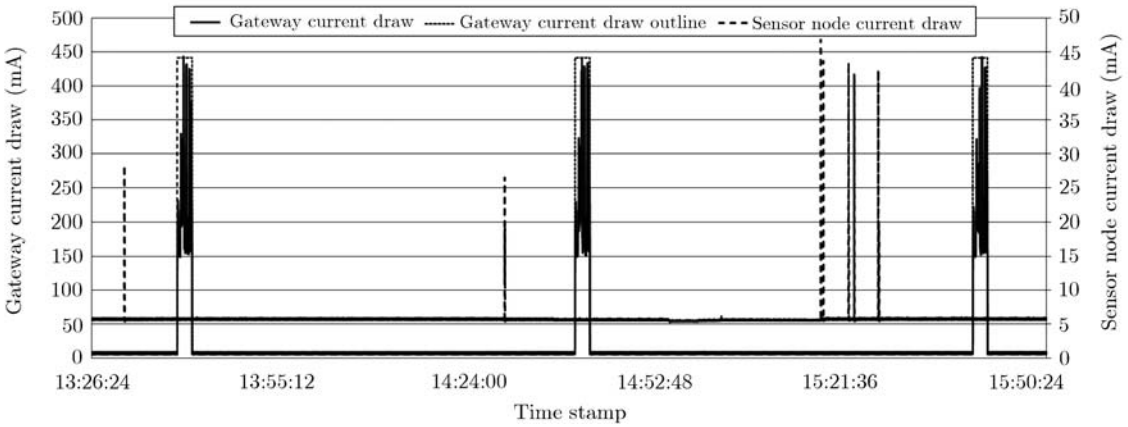

Figure 8 Current draw for a sensor node and the gateway with central node together through 10Ω load.

Table 4 Peak current, duration, frequency of each sensor node, central node and gateway during different operation modes

Current consumed by	Operation	Peak current (mA)	Duration (ms)	Frequency
Sensor node	Idle	6.20	If no operation	If no operation
	Sensor measurement and data Msg (no button pushed)	27.96	150	Every 1 h
	Sensor measurement and data Msg (button pushed)	46.36	450	If button pushed
Gateway	Turned off with central node idle or receiving Msg	8.67	If not turned on	If not turned on
	Turned on and uploading data	441.90	140 s	Every 1 h
Central node	Idle	0.08	If no operation	If no operation
	Data Msg (RX)	24.70	Less then 10	If Msg received
	Data Msg (TX)	49.40	30 per package	Every 1 h

PDUs which had field difference. During the tests, 246 pseudo PDUs were transmitted in about 45 min and the $N_{R,err}$ was 0%.

3.4 Power management strategy performance

Current consumed by a sensor node, the central node and gateway are shown in Figure 8 and Table 4. Since there was no routing table maintenance requirement for this network, a sensor node could stay in idle state mostly with a 6.20 mA current draw. The first two sensor node current draw impacts in Figure 8 were due to a scheduled measurement and data communication. The last five current draw impacts were caused by one of the buttons pressed to intrigue an immediate measurement or data upload which resulted in higher current consumption. The averaged power consumption of a sensor node was 5.71 mA at 3.3 V leading to 51.81 mW. Two sensor nodes brought 103.62 mW. Gateway current draw pulses were caused by the data-upload and field-to-web communication link establishment at each power loop. The averaged power consumption of the gateway with central node together was 14.51 mA at 12 V leading to 174.12 mW. At present, each power supply unit had sufficient ability to power two sensor nodes and the gateway with central node since the maximum averaged power consumed was 277.74 mW.

The 12 V, 12 A·h battery has energy supply ability of 144 W·h. Averaged power consumption of two sensor nodes and the gateway with central node together was 277.74 mW. Theoretically, the battery should be able to supply its corresponding powered components for 518 h (about 21 d) without charging.

4 Conclusions and discussion

This paper described the development of a two-tier hybrid sensor network system for un-supervised, real-time, in-field soil property monitoring and closed-loop irrigation control. Within the system, a

local wireless sensor network was developed to acquire soil properties include water content, electrical conductivity and temperature at different underground depths. A combination of cellular network and web-server worked together for performing data storage and querying to provide easy data access to final users everywhere through Internet. The average packet delivery rate and in-field data error rate, which were 84.76% and 0% respectively until day of test. The averaged valid data rate was above 97% in general for each sensor node.

The system has high flexibility and robustness in the data acquisition layer that: 1) new sensor nodes could added or removed without special re-configurations; 2) data were backed up in every single node as well as in the gateway; and 3) monitoring results could be uploaded manually in the field without cellular connections.

Future works may take the following issues into concern as: 1) currently, base node, central node and sensor stations are sharing one Node ID field within the PDU. Network expansion will be constrained, though seriously, since the Node ID space is limited. Extra PDU fields for separating cluster heads and members will be necessary; 2) there is no acknowledgement from central node to sensor station for each measurement data transmission which may lead to data loss.

Acknowledgements

This work was supported by Earmarked Fund for Modern Agro-industry Technology Research System of China, the National Natural Science Foundation of China (Grant No. 30871450), and the National Science Foundation of USA (Grant No. CNS-0709329).

References

1 Pierce F J, Elliott T V. Regional and on-farm wireless sensor networks for agricultural systems in Eastern Washington. Comput Electr Agric, 2008, 61: 32–43
2 López Riquelme J A, Soto F, Suardíaz J. Wireless sensor networks for precision horticulture in Southern Spain. Comput Electr Agric, 2009, 68: 25–35
3 Tacconi D, Miorandi D, Carreras I. Using wireless sensor networks to support intelligent transportation systems. Ad Hoc Netw, 2010, 8: 462–473
4 Fukatsu T, Hirafuji M, Kiura T. An agent system for operating Web-based sensor nodes via the Internet. J Robot Mechatr, 2006, 18: 186–194
5 Bellis S J, Delaney K, O'Flynn B, et al. Development of field programmable modular wireless sensor network nodes for ambient systems. Comput Commun, 2005, 28: 1531–1544
6 Green O, Nadimi E S, Blanes-Vidal V, et al. Monitoring and modeling temperature variations inside silage stacks using novel wireless sensor networks. Comput Electr Agric, 2009, 69: 149–157
7 Li Z, Wang N, Franzen A, et al. In-field soil property monitoring using a hybrid sensor network. In: Proceeding of ASABE Annual International Meeting 2009, Reno, NV, USA, 2009. 2950–2974
8 Huang X, Wang J, Fang Y. Achieving maximum flow in interference-aware wireless sensor networks with smart antennas. Ad Hoc Netw, 2007, 5: 885–896
9 Fariborzi H, Moghavvemi M. Architecture of a wireless sensor network for vital signs transmission in hospital setting. In: Proceeding of 2007 International Conference on Convergence Information Technology, Gyeongju, Korea, 2007. 745–749
10 King B A, Wall R W, Wall L R. Distributed control and data acquisition system for closed-loop site-specific irrigation management with center pivots. Appl Eng Agric, 2005, 21: 871–878
11 Coates R W, Delwiche M J. Wireless mesh network for irrigation control and sensing. Trans ASABE, 2009, 52: 971–981